

## II. MICROWAVE SPECTROSCOPY\*

Prof. M. W. P. Strandberg  
Prof. R. L. Kyhl  
Dr. B. D. Nageswara Rao  
J. M. Andrews, Jr.  
Y. H. Chu  
R. Huibonhoa

J. G. Ingersoll  
P. F. Kellen  
J. D. Kierstead  
S. H. Lerman  
J. W. Mayo

H. Pauwels  
Mahin Rahmani  
W. J. Schwabe  
G. J. Sehn  
J. R. Shane  
C. F. Tomes

### A. WORK COMPLETED

#### 1. SPIN-LATTICE RELAXATION IN PARAMAGNETIC CRYSTALS

This work has been completed by J. R. Shane and submitted as a thesis to the Department of Physics, M. I. T., May 10, 1963, in partial fulfillment of the requirements for the degree of Doctor of Philosophy. An abstract of the thesis follows.

A detailed investigation of the spin-phonon interaction for iron group spins at liquid-helium temperatures is presented. An effective interaction Hamiltonian for single phonon processes is used to describe the lattice-induced transitions between pairs of spin levels and the recovery of the energy level populations to thermal equilibrium.

The rate equations for spin-lattice relaxation are shown to follow directly from a density matrix formulation of the problem. The usual time-dependent perturbation theory expressions for the transition probabilities appear naturally in this formalism. Solutions of these equations are obtained for special magnetic field orientations for which direct relationships exist between the transition probabilities and the observed relaxation times.

A Green's function method is developed for calculating the matrix elements of the lattice operators that contribute to the interaction. This approach avoids the usual assumption that the normal lattice modes are unaffected by the presence of the paramagnetic impurities. The theory is applied to the phonon-impurity coupling in ruby, and the results are compared with the perfect lattice approximation. It is shown that the coupling is controlled by the defect states of the lattice, and these effects must be considered in order to obtain spin-phonon transition probabilities that have the observed frequency dependence.

Relaxation experiments at the symmetric orientation in ruby are described and the coefficients of the rank-two spin tensors that appear in the predicted form of the interaction are extracted from the data. An empirical interaction Hamiltonian is constructed with these coefficients and the frequency dependence that results from the Green's function method. This form of the interaction is used to calculate relaxation times at the

---

\*This work was supported in part by Purchase Order DDL B-00368 with Lincoln Laboratory, a center for research operated by Massachusetts Institute of Technology with the joint support of the U. S. Army, Navy, and Air Force under Air Force Contract AF19(604)-7400.

## (II. MICROWAVE SPECTROSCOPY)

90° orientation for several magnetic field values and temperatures. Good quantitative agreement with published relaxation measurements has been found.

### 2. NONLINEAR EFFECT OF LASER RADIATION ON METALS

This work has been completed by Y. H. Chu and submitted as a thesis to the Department of Physics, M. I. T., May 1963, in partial fulfillment of the requirements for the degree of Bachelor of Science. An abstract of the thesis follows.

An attempt was made to observe the optical nonlinear effect from the interaction of the ruby laser radiation and the surface of metals, in particular, the generation of second harmonics of the laser frequency by the metal. By using a crude free-electron theory, this phenomenon had a minimum theoretical effective cross section of  $2 \times 10^{-32} \text{ cm}^2$ . The electric fields that are necessary to allow the second-order components of the induced dipole are much greater than those in insulators and semiconductors. After 30 experiments in which samples of copper and aluminum were used, no positive effect was observed. Detection was accomplished by photographic emulsion, which had an experimental minimum detectability of 1,000 photons.

### 3. THE OPERATION AND MODE SPECTRUM OF A CONFOCAL RESONANCE CAVITY AT 23,870 mc WITH A CONSIDERATION OF THE AMMONIA ABSORPTION COEFFICIENT

This work has been completed by C. F. Tomes and submitted to the Department of Physics, M. I. T., May 1963, as a thesis in partial fulfillment of the requirements for the degree of Bachelor of Science. An abstract of the thesis follows.

A confocal resonator with spherical ends ( $b=16.2 \text{ cm}$ ) was constructed and operated in the K-band microwave region around 23,870 mc. The nondegenerate mode spectrum was fully explained by having different eigenfunctions for the  $m$  and  $n$  values. In removing this last degeneracy in  $m$  and  $n$ , the split of 7 mc (independent of separation) was found to correspond to a difference of 4 mm in radii of curvature. Near the confocal separation a high-loss region was seen to be just as predicted by these different curvatures. Because of technical problems, determination of the ammonia absorption coefficient was not possible.

M. W. P. Strandberg

## B. ULTRASONIC ATTENUATION IN SUPERCONDUCTORS

Measurements of ultrasonic attenuation in superconducting metals have been extended to the L-band region. The experiment<sup>1</sup> is identical to that carried out at 165 mc except for certain changes in the equipment. The transmitter is a modified General Radio Unit Oscillator. The dc plate supply lead has been disconnected and 1200-volt dc pulses of

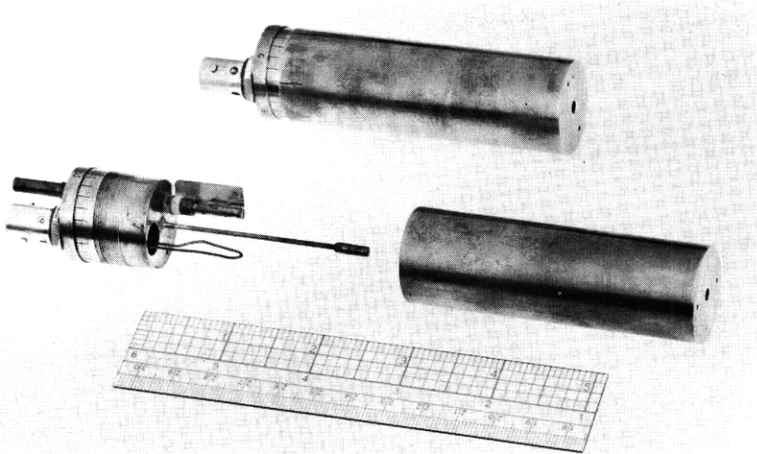


Fig. II-1.

Re-entrant cavities used for the L-band transmitting and receiving transducers.

0.5- $\mu$ sec duration obtained from an external source are applied to the plate of the oscillator tube. The oscillator provides approximately 25 watts of peak power. The re-entrant cavities are shown in Fig. II-1. Coarse tuning is achieved by rotating the barrel; this operation changes the gap length between the end of the post and the end wall of the cavity in which the quartz rod is inserted. Also, a fine-tuning control is included in one of the cavities, which consists of a small vane that can be rotated through  $180^\circ$  with respect to the rf magnetic field within the cavity. This provides a means of matching the resonant frequencies of the cavities while they are at helium temperature. In all other respects the details of the experiments are similar to those reported earlier.<sup>1</sup>

Interaction of 1 kmc coherent phonons with incoherent thermal phonons at room temperature is quite pronounced. The result is that with our equipment it is never possible to see more than five or six acoustic echoes in 1/2-inch quartz rods at room temperature; however, the number of observable echoes at 4.2°K is around 100. The attenuation coefficient in quartz,  $a_q$ , was measured at both temperatures at 0.89 kmc: at 300°K,  $a_q = 4.3$  db/cm; at 4.2°K,  $a_q = 0.98$  db/cm. The phonon-phonon scattering is negligible at 4.2°K, so that the 0.98 db/cm was considered to be the residual temperature-independent loss resulting from lattice defects and geometrical effects. This residual attenuation was subtracted from both measurements, and the resulting 3.3 db/cm was compared with, and found to be consistent with, the temperature-dependent phonon-phonon scattering reported by Jacobsen, Bömmel, and Dransfeld.<sup>2</sup>

Attention was then turned to the measurement of the difference in the electronic contribution to the ultrasonic attenuation coefficient between normal and superconducting indium. Three samples of indium of varying thickness were sandwiched between quartz rods, and the height of the transmitted acoustic pulses was measured as a function of external magnetic field.

## (II. MICROWAVE SPECTROSCOPY)

Sample 1

Thickness:  $0.015 \text{ cm} \pm 0.001$

$T = 1.9^\circ\text{K} \pm 0.1^\circ\text{K}$

The transmitted pulses are shown in Fig. II-2a for the normal state and in Fig. II-2b for the superconducting state. The pulse denoted  $a_0$  is rf leakage from the transmitter. The pulse denoted  $a_1$  is the first acoustic pulse that has traversed the sample. The pulse denoted  $a_2$  is a superposition of two acoustic pulses: one has made a double reflection in the first rod; the other, a double reflection in the second rod. The superposition is caused by the fact that the two quartz transducer rods are equal in length (within  $\pm 0.001$  in.). The pulse denoted  $\Delta$  is an rf calibration pulse controlled by a calibrated attenuator and variable delay, which has been introduced into the system for the purpose of measuring the height of the acoustic pulses. The pulse denoted  $a_3$  is a superposition of three acoustic pulses: one has made four reflections in the first rod, another has made a double reflection in the first rod and a double reflection in the second rod, and the third has made four reflections in the second rod. Since  $a_3$  was the largest pulse, measurements of the magnetic field dependence of the ultrasonic attenuation coefficient were made on it alone. These results are plotted in Fig. II-3. The difference in magnitudes of the other pulses are also shown for comparison.

As mentioned in an earlier report<sup>1</sup> ( $a_n - a_s$ ) can probably not be measured from any pulses other than the first because of the unknown phase relationships between the various pulses forming the superpositions. The exact cause of the phase changes between these pulses as the sample is switched between the superconducting and the normal states is not understood, but the existence of such an effect seems to be the best explanation for the discrepancies in ( $a_n - a_s$ ) shown in Fig. II-3.

The magnetic field dependence of ( $a_n - a_s$ ) for this sample supports the contention stated previously<sup>1</sup> that the shape of the curve is characteristic of the intermediate state. Note the very sharp transition at  $(H_c)_{\text{exp}}$ . This indicates that there is virtually no region of the magnetic field where this sample is in the intermediate state. As previously given<sup>3</sup>  $H_e/H_c = 1 - n$ . Our data indicate that  $H_e \approx H_c$ , and we conclude that  $n = 0$  for Sample 1. For any given body the sum of the demagnetizing coefficients ( $4\pi n$ ) for any three mutually perpendicular axes is  $4\pi$ . Since  $n=1$  for a thin plane disc with its surface normal to the magnetic field,  $n = 0$  for a disc with its surface parallel to the magnetic field. The ratio of the diameter to the thickness of Sample 1 is 20, and therefore the agreement with the macroscopic theory of the intermediate state is excellent. The values  $[H_c(T)]_{\text{calc}}$  shown in Figs. II-3, II-5, and II-7 were obtained from the well-known deviations of superconducting critical fields from the parabolic law.

Measurements of  $a_n$  in a sample as thin as this are likely to be unreliable for two reasons. First, the magnitude of the change in pulse height is so small that it introduces appreciable error. (Compare  $a_2$  in Fig. II-2a and 2b.) The second is that it is quite

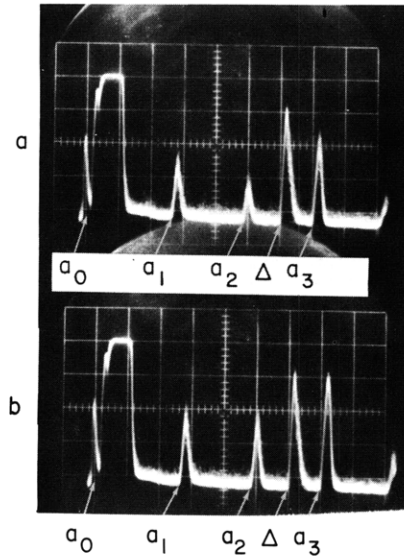


Fig. II-2. (a) Ultrasonic pulses at L-band transmitted through Sample 1 of indium in the normal state.  $a_0$  is rf leakage;  $a_1$ , the first transmitted pulse;  $a_2$ , a superposition of two reflected pulses;  $\Delta$ , a calibration pulse;  $a_3$ , a superposition of three reflected pulses (scale,  $2 \mu\text{sec/cm}$ ).  
 (b) Same as in (a) except that the sample is in the superconducting state.

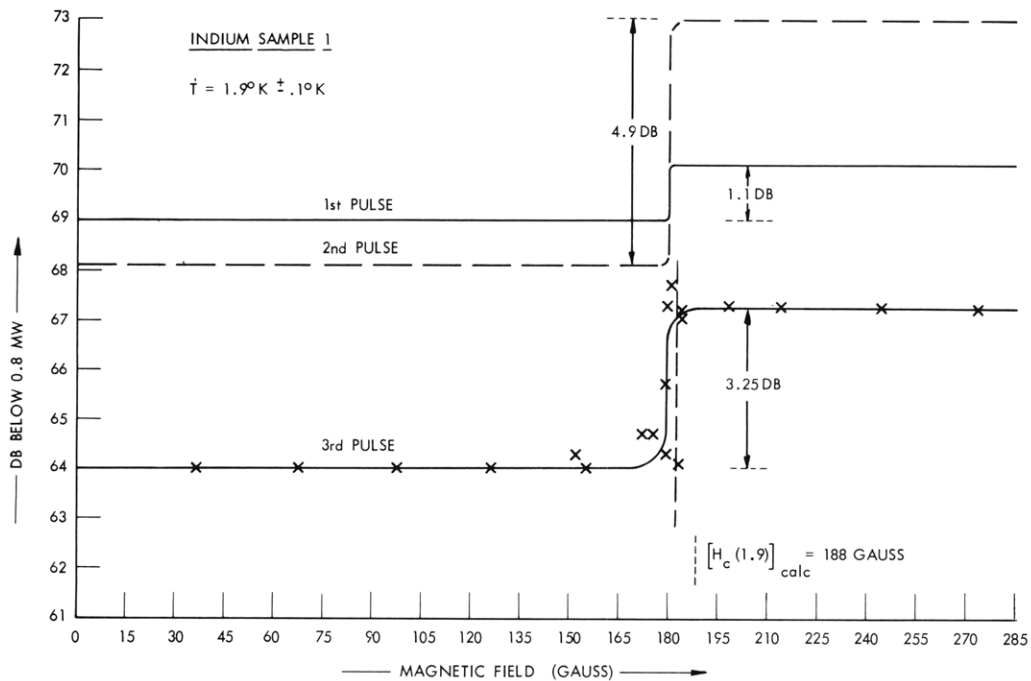


Fig. II-3. Attenuation of L-band ultrasonic pulses in Sample 1 of indium plotted as a function of external magnetic field. Experimental points were taken only on the third pulse.

## (II. MICROWAVE SPECTROSCOPY)

possible that multiple reflections are taking place in such a thin sample. Multiple reflections have never been observed in samples thick enough for them to be resolved. On the other hand, Sample 1 is so thin (1/18 of the pulse length) that up to 10 reflections could take place without noticeable pulse broadening. However, setting these objections aside for the moment, we tentatively calculate  $a_n$  for Sample 1, using the formula given previously.<sup>4</sup>

$$(a_n)_{\text{exp}} \approx 17 \text{ cm}^{-1} \quad (\text{tentative value}).$$

From the Pippard theory for ultrasonic attenuation in metals at low temperatures  $a'$ , evaluated at 910 mc, is

$$(a')_{\text{th}} = 23 \text{ cm}^{-1} \quad ql \gg 1,$$

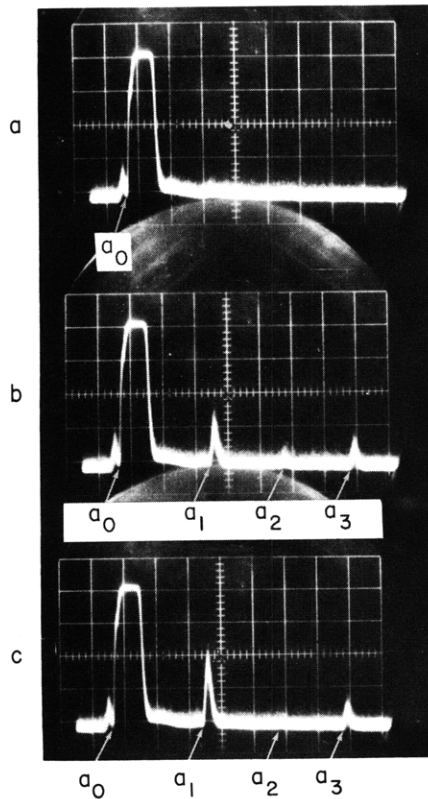


Fig. II-4. (a) Ultrasonic attenuation at L-band in Sample 2 of indium in the normal state. No observable acoustic energy traverses the sample. (b) Same as (a), but in the intermediate state. Note the pulse  $a_2$ , made up of the superposition of the two double reflections. The appearance of this pulse was a random function of the manner in which the magnetic field was changed. (c) Same as (a), but in the superconducting state. Note that  $a_2$  has almost entirely disappeared.

(II. MICROWAVE SPECTROSCOPY)

where  $a'$  denotes the limiting value of the electronic contribution to the ultrasonic attenuation coefficient for long electronic mean-free path.

Note that in all of the measurements on indium reported here, the temperature of the sample was sufficiently low that the superconducting energy gap had opened up to a value very close to its value at absolute zero. That is, the energy-gap factor<sup>4</sup>  $\tanh \left[ \frac{\epsilon(T)}{2kT} \right]$  was very nearly equal to unity. This means that when the sample is switched from the superconducting to the normal state we observe very nearly the full effect on the ultrasonic attenuation that is due to the conduction electrons.

Sample 2

Thickness: 0.208 cm  $\pm$  0.001

T = 1.8°K  $\pm$  0.1°K

Figure II-4 shows the acoustic pulses transmitted through this sample. Figure II-4a shows that in the normal state no transmitted sound can be observed above the noise.

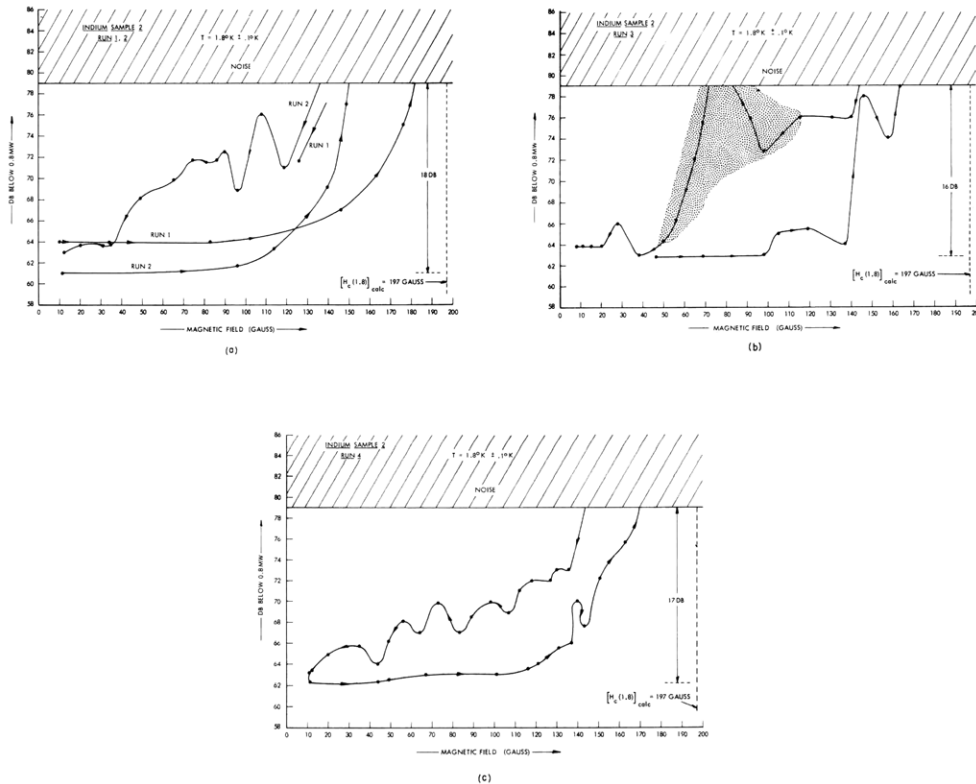


Fig. II-5. Attenuation of L-band ultrasonic pulses in Sample 2 of indium plotted as a function of external magnetic field. The shaded area shown in (b) indicates a region of extreme instability where the pulse height fluctuated even while the magnetic field was held constant.

## (II. MICROWAVE SPECTROSCOPY)

In Fig. II-4b the sample is in the intermediate state; in Fig. II-4c, the superconducting state. The pulse denoted by  $a_2$  represents just such a superposition of pulses as discussed with respect to Sample 1. Note that this pulse appears here only in the intermediate state. Its appearance was not reproducible, sometimes appearing momentarily and then disappearing altogether. At other times, it could be displayed for long periods of time. Its magnitude seemed to depend to some extent on the speed at which the magnetic field was varied and on other details of the traversal through the intermediate state. The behavior of this pulse seemed to indicate some sort of instability that characterized the sample while in the intermediate state. It is thought that the height of this pulse may be determined by the phase relationship between the individual pulses composing the superposition. These phase differences, in turn, may be caused by the structure of the intermediate state which allows acoustic energy to pass through different sections of the sample, the thickness of the sample possibly varying by one or more acoustic wavelengths over the diameter of the quartz transducer rods.

Such instability was even more evident in the magnetic field dependence of the ultrasonic attenuation and can be seen in the plots shown in Fig. II-5. Note that the actual structure of the curve seems to be quite random. In some cases, especially during run 3, a good deal of instability in the pulse height could be observed when the magnetic field was not being altered at all. The instability effects, however, were usually sufficiently well correlated with magnetic field changes to rule out instrumentation difficulties. The shaded portion of the curve in Fig. II-5b represents a region of extreme instability. Each run, however, showed a reproducible hysteresis effect. Similar effects have been observed by other investigators in polycrystalline tin and lead.<sup>6, 7</sup> This behavior has been attributed to the trapping of magnetic flux in the center of the sample which causes a persistence of the intermediate state as the magnetic field decreases.

We should point out one feature of these observations. We are working with such a combination of high frequency and thick sample that the total change in attenuation ( $\alpha_n - \alpha_s$ ) between the normal and the superconducting state is very large. Thus when the sample is in the normal state, the fraction of the acoustic power reaching the receiver is of the order of one one-hundredth that which is passed while the sample is in the superconducting state. The obvious disadvantage of these conditions is that the total change in attenuation could not be measured in this sample. However, one distinct advantage is that small fluctuations of the ultrasonic attenuation coefficient of the metal are greatly magnified in the intermediate state. Thus it is possible that such techniques may provide detailed information concerning the kinetics of the superconducting transition process as the metal passes through the intermediate state.

Although this sample was too thick for us to measure the total change in the ultrasonic attenuation coefficient between the normal and the superconducting states, we can conclude that it is somewhat greater than 18 db. Since the pulse entered the noise close



(II. MICROWAVE SPECTROSCOPY)

to the critical field, most of the change may have been observed. Again, we tentatively calculate the value of the attenuation coefficient  $\alpha_n$  for Sample 2.<sup>4</sup>

$$(\alpha_n)_{\text{exp}} \cong 20 \text{ cm}^{-1} \quad (\text{estimated value}).$$

Sample 3

Thickness:  $0.127 \text{ cm} \pm 0.001$

$T = 2.0^\circ\text{K}$  and  $1.8^\circ\text{K} \pm 0.1^\circ\text{K}$

Figure II-6a, 6b, and 6c shows the pulses transmitted through Sample 3 in the superconducting, intermediate, and normal states, respectively. They are denoted  $a_1$ ,  $a_2$ , and  $a_3$ :  $a_0$  is rf leakage from the transmitter. The origin of the tiny pulse denoted  $b$  (just before  $a_1$ ) is unknown. Its position indicates that if it is an acoustic pulse that passed through the sample, its velocity must have been much greater than the usual velocity of

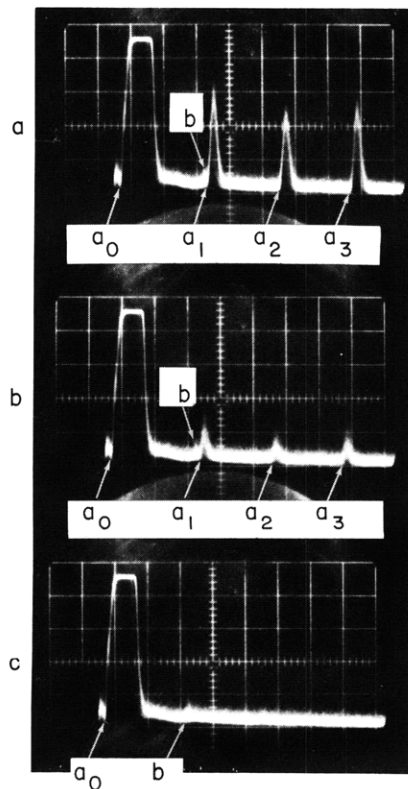
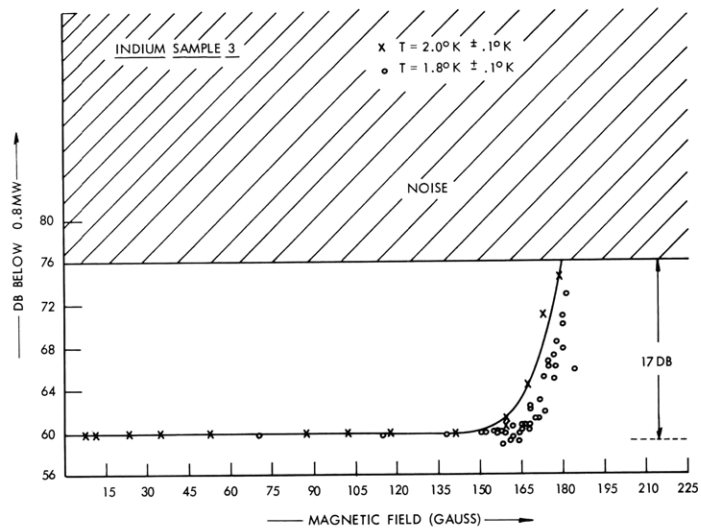
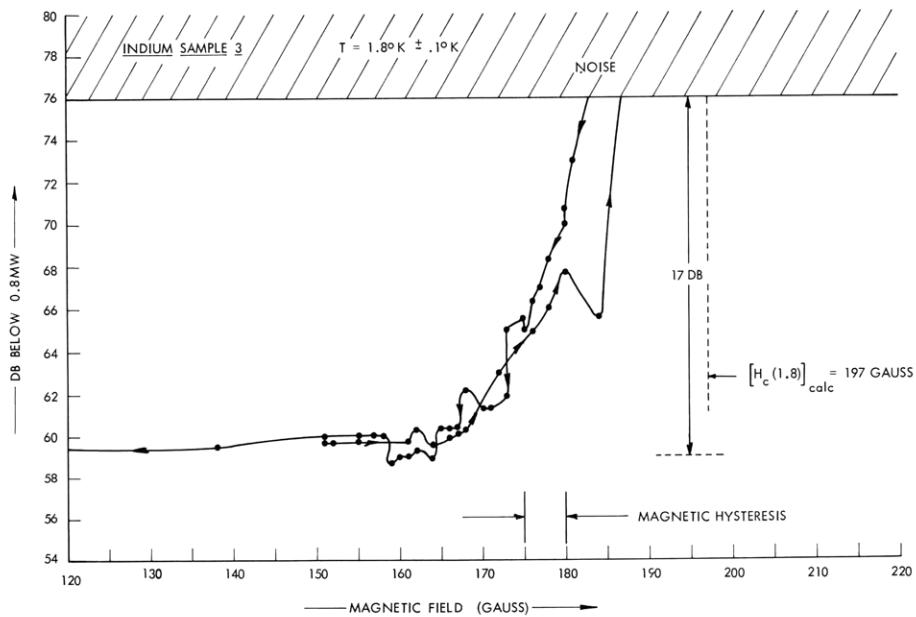


Fig. II-6. (a) Ultrasonic pulses at L-band transmitted through Sample 3 of indium in the superconducting state.  
(b) Same as (a), but in the intermediate state.  
(c) Same as (a), but in the normal state. The a's have disappeared entirely. Note the tiny pulse, denoted  $b$ . Its origin is unknown, but if it is an acoustic pulse it has a velocity much greater than that of the longitudinal mode denoted by the a's.



(a)



(b)

Fig. II-7. (a) Attenuation of L-band ultrasonic pulses in Sample 3 of indium plotted as a function of external magnetic field. Note the absence of the superconducting hysteresis effect.  
 (b) Expanded view of the points for  $T = 1.8^\circ\text{K}$ , plotted in (a), showing the details of the magnetic path through the intermediate state. If any superconducting hysteresis exists it would be masked by the hysteresis of the external magnet.

longitudinal ultrasonic waves in indium, which is 2.72 km/sec along the 100 axis at 4.2°K.<sup>8</sup> It is not known whether our samples were single crystals; however, the orientation dependence of the velocity of the longitudinal mode is small,<sup>8</sup> and our samples were so thin that accurate velocity determinations were not possible.

The data taken on the magnetic field dependence of the ultrasonic attenuation coefficient show no large hysteresis effects. This is evident in Fig. II-7. The spread in the data occurs throughout a region that is so narrow that much of it should probably be attributed to hysteresis in the iron of the external electromagnet, which may have been as much as 5 gauss. However, the magnitude of this uncertainty was sufficiently small that no attempt was made to correct for magnetic hysteresis in any of the data. Again, the bond was too thick to obtain a determination of the entire change in the attenuation ( $a_n - a_s$ ), but data were taken up to a magnetic field of approximately 182 gauss, which was the field in which the sharp superconducting transition occurred for Sample 1. Consequently, this is probably the most reliable data taken thus far from which  $a_n$  at 910 mc can be estimated. We obtain<sup>4</sup>

$$(a_n)_{\text{exp}} = 28 \text{ cm}^{-1} \quad (\text{estimated value}).$$

The most puzzling aspect of the data taken for Samples 2 and 3 is the pronounced difference in the superconducting hysteresis effects. The samples were prepared from the same source, and their exterior dimensions did not differ greatly. Not much information, however, is known about the details of the acoustic path through the sample. That these effects are important in the observation of superconducting hysteresis effects has been demonstrated by Mackinnon.<sup>6</sup>

The author is indebted to John Kierstead for technical assistance with the pulse-forming circuit, and to E. C. Ingraham for the construction of the L-band cavities.

J. M. Andrews, Jr.

#### References

1. J. M. Andrews, Jr., Ultrasonic attenuation in superconductors, Quarterly Progress Report No. 69, Research Laboratory of Electronics, M. I. T., April 15, 1963, pp. 1-9.
2. E. H. Jacobsen, Experiments with phonons at microwave frequencies, Quantum Electronics, edited by C. H. Townes (Columbia University Press, New York, 1960), p. 468.
3. J. M. Andrews, Jr., op. cit., p. 8, Eq. 7.
4. Ibid., p. 7, Eq. 5.
5. A. B. Pippard, Phil. Mag. 46, 1104 (1955).
6. L. Mackinnon, Phys. Rev. 106, 70 (1957).
7. H. E. Bömmel, Phys. Rev. 96, 220 (1954).
8. B. S. Chandrasekhar and J. A. Rayne, Phys. Rev. 124, 1011 (1961).

